Proceedings of the 30th International Cosmic Ray Conference
Rogelio Caballero, Juan Carlos D'Olivo, Gustavo Medina-Tanco,
Lukas Nellen, Federico A. Sánchez, José F. Valdés-Galicia (eds.)
Universidad Nacional Autónoma de México,
Mexico City, Mexico, 2008
Vol. 4 (HE part 1), pages 131–134

ID 825

30TH INTERNATIONAL COSMIC RAY CONFERENCE

ICRC'07 Mérida, México

Investigations of the lateral extension of radio emission in air showers by LOPES30 measurements

S. NEHLS[a], W.D. APEL[a], J.C. ARTEAGA[a], T. ASCH[b], J. AUFFENBERG[c], F. BADEA[a], L. BÄHREN[d], K. BEKK[a], M. BERTAINA[e], P.L. BIERMANN[f], J. BLÜMER[a,g], H. BOZDOG[a], I.M. BRANCUS[h], M. BRÜGGEMANN[i], P. BUCHHOLZ[i], S. BUITINK[j], H. BUTCHER[d], A. CHIAVASSA[e], F. COSSAVELLA[g], K. DAUMILLER[a], V. DE SOUZA[g], F. DI PIERRO[e], P. DOLL[a], R. ENGEL[a], H. FALCKE[d,j], H. GEMMEKE[b], P.L. GHIA[k], R. GLASSTETTER[c], C. GRUPEN[i], A. HAUNGS[a], D. HECK[a], J.R. HÖRANDEL[j], A. HORNEFFER[j], T. HUEGE[a], P.G. ISAR[a], K.-H. KAMPERT[c], D. KICKELBICK[i], Y. KOLOTAEV[i], O. KRÖMER[b], J. KUIJPERS[j], S. LAFEBRE[j], P. LUCZAK[l], H.J. MATHES[a], H.J. MAYER[a], C. MEURER[a], J. MILKE[a], B. MITRICA[h], C. MORELLO[k], G. NAVARRA[e], A. NIGL[j], J. OEHLSCHLÄGER[a], S. OSTAPCHENKO[a], S. OVER[i], M. PETCU[h], J. PETROVIC[j], T. PIEROG[a], S. PLEWNIA[a], J. RAUTENBERG[c], H. REBEL[a], M. ROTH[a], H. SCHIELER[a], O. SIMA[m], K. SINGH[j], M. STÜMPERT[g], G. TOMA[h], G.C. TRINCHERO[k], H. ULRICH[a], J. VAN BUREN[a], W. WALKOWIAK[i], A. WEINDL[a], J. WOCHELE[a], J. ZABIEROWSKI[l], J.A. ZENSUS[f].
[a] *Institut für Kernphysik, Forschungszentrum Karlsruhe, Germany*
[b] *Inst. Prozessdatenverarbeitung und Elektronik, Forschungszentrum Karlsruhe, Germany*
[c] *Fachbereich Physik, Universität Wuppertal, Germany*
[d] *ASTRON, Dwingeloo, The Netherlands*
[e] *Dipartimento di Fisica Generale dell'Università Torino, Italy*
[f] *Max-Planck-Institut für Radioastronomie Bonn, Germany*
[g] *Institut für Experimentelle Kernphysik, Universität Karlsruhe, Germany*
[h] *National Institute of Physics and Nuclear Engineering Bucharest, Romania*
[i] *Fachbereich Physik, Universität Siegen, Germany*
[j] *Dept. of Astrophysics, Radboud University Nijmegen, The Netherlands*
[k] *Istituto di Fisica dello Spazio Interplanetario, INAF Torino, Italy*
[l] *Soltan Institute for Nuclear Studies Lodz, Poland*
[m] *Department of Physics, University of Bucharest, Romania*
steffen.nehls@ik.fzk.de

Abstract: The antenna field of LOPES uses inverted V-shaped dipole antennas to measure radio signals originating from extensive air showers (EAS). The LOPES antennas are measuring in coincidence with the air shower experiment KASCADE-Grande. For roughly one year data in the frequency range from 40–80 MHz were taken, having 30 linearly polarized antennas oriented to East-West. In this data set the East-West polarization only was measured in order to investigate in detail the lateral extension of the radio emission. By using an external source all antennas have an absolute amplitude calibration, i.e. a frequency dependent correction factor allows to reconstruct the electric field strength of the radio emission. For first analyses, in particlular air showers with a high signal-to-noise ratio, data are used to investigate the lateral distribution, which shows an exponential decrease.

Introduction

The LOPES experiment was set up at the site of KASCADE-Grande [1] to confirm the principle of radio detection of air showers [2] and the theory of geosynchrotron radiation [3] as dominant emission process in the frequency range below a few hundred Megahertz. The KASCADE-Grande experiment is measuring EAS in the energy range 10^{14}–

10^{18} eV. LOPES and KASCADE-Grande experiment are measuring in coincidence the radio emission of EAS, implemented by an external triggering for LOPES. The LOPES experiment uses inverted vee-shaped dipole antennas. For the detection of radio signals from 40 to 80 MHz was chosen in order to avoid most of the radio frequency interference (RFI) being present at the location.

In a first construction phase (LOPES10), 10 antennas were taking a sufficiently large data set for detailed investigations [2] of the relation between detected radio pulses and air shower reconstruction parameters, provided by KASCADE-Grande.
In a next construction phase (LOPES30), the number of antennas and the baseline were increased. In addition an absolute amplitude calibration was performed to reconstruct the electric field strength at each individual antenna. For both phases only the East-West polarization direction was measured. Meanwhile in a third phase dual polarization measurements are performed.

Calibration

The amplitude calibration uses a reference source (VSQ) of known electric field strength at a certain distance. Each LOPES30 radio antenna is calibrated at its location inside the KASCADE-Array and therefore this calibration includes all environmental effects, like ground characteristics, temperature effects, or setup systematics. The power to be received from the radio antenna in calibration mode is compared with the power recorded in the LOPES electronics P_{M}. With the relation:

$$V(\nu) = \left(\frac{4\pi r\nu}{c}\right)^2 \cdot \frac{P_M(\nu)}{G_r(GP)_{VSQ}\cos^2(\beta)} \quad (1)$$

The amplification factor $V(\nu)$ describes the frequency dependent behavior of each electronic channel for the signal transmission. The directivity pattern G_{r} of the LOPES antenna is obtained by a simulation assuming realistic conditions. To quantify polarization losses during a misalignment of the linearly polarized VSQ and linearly polarized LOPES antenna the angle β is introduced. For the VSQ only the product of gain and emitted power $(GP)_{\mathrm{VSQ}}$ is known. In Figure 1 the determined amplification factors $V(\nu)$ for a vertical calibration for all 30 antennas are shown.

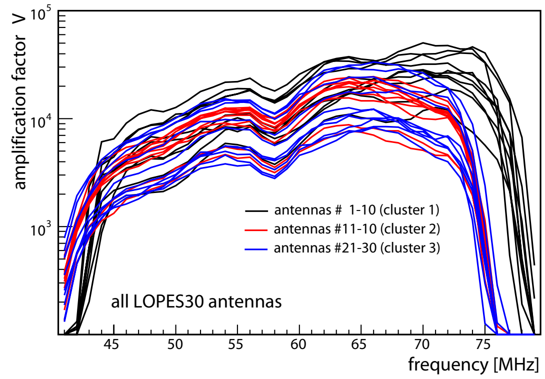

Figure 1: The frequency dependent amplification factors for all 30 antennas obtained by the amplitude calibration.

The earlier LOPES10 hardware can be distinguished (antennas 1–10) by their band pass range (43–76 MHz) from the other 20 antennas (42–74 MHz). The calibration results in a spread for the amplification factors of nearly one order of magnitude. This large spread illustrates the need for an absolute calibration and is corrected for in the analysis software. The uncertainty of the calibration method can be estimated from repeated measurement campaigns for a single antenna under all kinds of conditions, including the precision of achieving the same geometry in all measurements. It results in an uncertainty of approximately 25% for the power related amplification factor V, averaged over the effective frequency range.

Radio pulse investigations

LOPES30 in the described setup took data in the period from mid of November 2005 until beginning of December 2006, receiving 966.000 external triggers from KASCADE. The LOPES data acquisition system was able to process 860.000 of them, where the loss is mostly due to the dead-time of roughly 1.5 seconds.

The EAS observables, e.g. shower size, number of muons, arrival direction, and shower core position are reconstructed only with the KASCADE data and have to fulfill quality cuts, before further processing of the radio information. As the full data set consists mostly of low energetic showers the expected radio signal strength is relatively low.

Therefore, for a first radio pulse analysis a preselection of high energetic showers based on restrictions in the electron and muon number was done. Showers with shower size $N_\mathrm{e} > 5 \cdot 10^6$ and truncated muon number[1] $N_\mu^\mathrm{tr} > 5 \cdot 10^4$ where further investigated, giving 1200 candidate events.

The analysis of the candidate events performs a series of processing steps to determine the correlation quantity cc-beam pulse height. First the raw data is corrected for instrumental delays and afterwards a fast Fourier-transformation is applied. To suppresses radio frequency interference a mitigation of narrow band emitters is applied. Then the reconstructed geometry of the EAS from KASCADE is taken to apply a phase shift to each antenna data, what can be translated as a shift in time. Further the amplitude calibration is considered and a correction due to small instrumental phase shifts. The data are transformed back into the time domain, according to the observables from the EAS reconstruction. All time series $s_i(t)$ can now be superimposed interferometrically and with:

$$CC(t) = \pm \sqrt{\left| \frac{1}{N_{pairs} - 1} \sum_{i \neq j} s_i(t) \cdot s_j(t) \right|} \quad (2)$$

the so called cross correlation beam $CC(t)$ is calculated. With this kind of data processing the radio pulses recorded in the LOPES30 data can be identified. For a detailed description of the processing steps see [4].

Such cc-beam radio pulses are fitted with a Gaussian function to quantify the height, which is an averaged field strength for a mean distance to the shower axis of the selected radio antennas. As an estimation of the pulse height uncertainty the uncertainty of the Gaussian fit is used. For 849 candidates a radio pulse could be fitted (see Figure 2).

From Monte Carlo simulations an approximately linear dependence of primary energy E_0 with the electric field strength E is predicted. As the number of muons detected at ground scales roughly with the primary energy, in Figure 2 the radio pulse height is plotted against the truncated number of muons N_μ^tr. The used error bars are derived from the fit uncertainty.

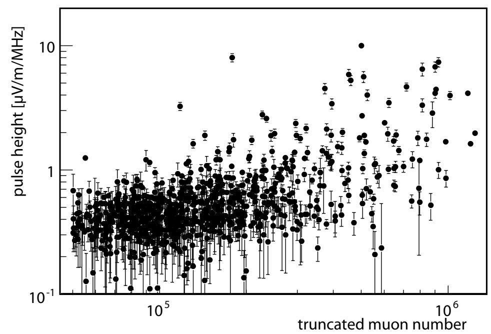

Figure 2: Relation of truncated muon number N_μ^tr and cc-beam pulse height.

	Shower 1	Shower 2
$\log N_\mathrm{e}$	7.26	7.27
$\log N_\mu^\mathrm{tr}$	5.95	5.91
$\log E_\mathrm{est.}$ [eV]	17.4	17.4
θ [deg.]	24.0	23.8
ϕ [deg.]	2.3	4.9
CC_all [μV/m/MHz]	6.8 ± 0.6	6.5 ± 0.8

Table 1: EAS observables for two similar shower.

There can be seen no significant correlation between those two quantities. Due to the strong dependence of the radio signal on the shower direction [5] (geomagnetic angle, zenith angle, and azimuth angle) and on the distance to the shower core, the correlation with the muon number is spread out and an unfolding of the dependences is needed. In a first step for this unfolding the lateral dependence will be investigated in more detail and discussed here for two events explicitly.

Lateral extension of radio signals

In the used data set there are two resembling showers, which can be used to directly compare the radio pulse height for certain distance ranges from the shower axis. The layout in Fig. 3 gives the shower core position in the KASCADE-Array and the originating direction indicated by an arrow. The reconstructed EAS observables are given in Table 1 in addition to the cc-beam of all antennas (CC_all) (see Fig. 4), we considered antennas

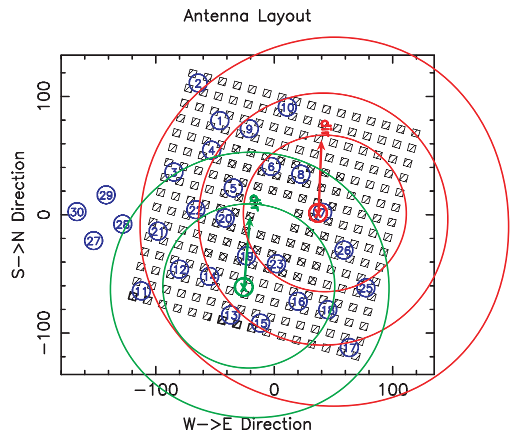

Figure 3: The radial distance ranges are illustrated by rings around the shower core, indicated with an encircled X. Green-left: 3 distance ranges; Red-right: 4 distance ranges. Ranges are from 0–50 m, 50–100 m, 100–150 m, 150–200 m.

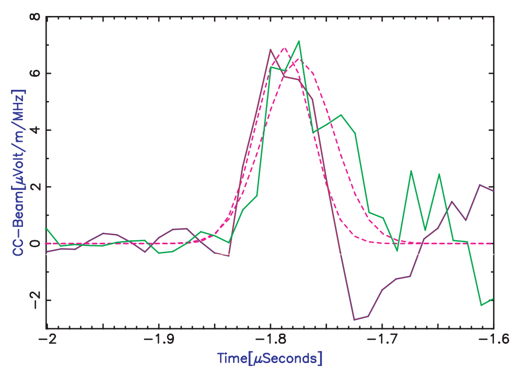

Figure 4: Combined cc-beam plot (solid lines, light and dark) with Gaussian fit (dashed lines) for complete antenna field.

within 0–50, 50–100, 100–150 m, and further out from the shower axis and the calculated cc-beams pulse heights are shown in Figure 5. The simulation and earlier data analyses predict an exponential decrease of the radio field strength E with increasing lateral distance R. Following the relation: $E \sim \exp(-R/R_0)$, the shown fit is performed for both events and radial distances larger then 50 m, resulting in a scaling parameter $R_0 = 101 \pm 43$ m. Due to increasing RFI from the surrounding detector stations close to the shower core, the cc-beam pulse height in the innermost ring can by systematically affected towards lower values, but both events have similar field strengths further out.

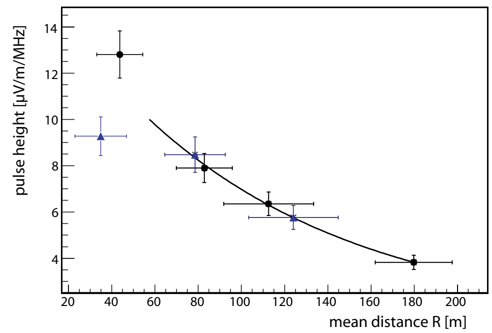

Figure 5: Lateral distribution of the radio pulse height for sub-sets of antennas. The events are fitted by an exponential function $\exp(-R/R_0)$.

Conclusions

The investigations of the lateral distribution of the radio emission with LOPES30 data are performed with absolute amplitude calibrated antennas. The spread of one order of magnitude in the amplification factor is corrected for in the analysis software and a systematic uncertainty of $\approx$ 13% for measured field strengths remains.

Exemplarily two high energy events with high S/N ratio are investigated for there lateral distribution. The reconstruction of the cc-beam radio pulse height was done for distance ranges of round 50 m from the shower axis. The exponential decrease as predicted by the simulations is verified and a scaling parameter R_0 could by determined for the relation $E \sim \exp(-R/R_0)$ to $R_0 = 101 \pm 43$ m. A full analysis of the LOPES30 data set in terms of lateral behavior of the radio signal is currently in preparation.

References

[1] T. Antoni et al., Nucl. Instr. Meth. A, Vol. 513, 490 (2003)

[2] H. Falcke et al., Nature 435, 313 (2005)

[3] T. Huege & H. Falcke, APh. Vol. 24, 116, (2005)

[4] A. Horneffer et al., Int. J. Mod. Phys., Vol. A21S1, 168 (2006)

[5] A. Haungs et al., Proc. ARENA conf., Newcastle, UK; Int. J. Phys.: Conf. Series (2006)